

Numerical Simulation on Combustion Characteristics of a Pulverized Biomass Swirl Burner

Niwat Suksam, Chinnapat Turakarn, and Jarruwat Charoensuk*

Department of Mechanical Engineering, Faculty of Engineering, King Mongkut's Institute of Technology Ladkrabang,
Chalongkrung Road, Ladkrabang, Bangkok, 10520, Thailand

* Corresponding Author: E-mail kcjaruw@kmitl.ac.th, Tel. 0 2329 8350-1, Fax: 0 2329 8352

Abstract

Numerical simulation of pulverized biomass combustion in a laboratory swirl burner was carried out aiming to investigate the effect of swirl number on combustion characteristics. Discrete phase model and eddy-dissipation model were adopted to represent combustion behavior of char particle and volatile in flue gas domain. Effects of five swirl numbers ranging from 0.8 to 1.2 were investigated. The results show that combustion characteristics such as the flow velocity, pressure, temperature and distributions of species were strongly dependent on the swirl number. Combustion appeared to be more intensified when increasing the swirl number. Complete combustion of volatile could be achieved within the domain of furnace at swirl number 1.2 while it was most likely that additional length of furnace was required at lower swirl number. However pressure loss factor increased significantly with swirl number starting from 0.35 at swirl number 0.8 and increased up to 0.9 at swirl number 1.2.

Keywords: Biomass combustion, Swirl flame, CFD.

1. Introduction

The over-consumption of coal has become a debatable issue over the years. As coal is non-renewable energy, it is likely that its supply and price are unpredictable. Due to the concern on the impact of emission from coal and global warming, biomass is an interesting renewable and sustainable resource of energy. Biomass is carbon neutral fuel. However, biomass has low calorific value because the mixture of biomass has lower carbon content than coal. Therefore, in converting chemical energy to thermal energy by combustion, one should consider its thermal performance and flame stability for sufficient use in the process.

The pulverized biomass is a fuel for pure biomass combustion or co-firing with pulverized coal in the furnace of industrial boiler for power generation and process steam. Swirl flow is an essential constitution for combustion performance and stability. Most burners used in industrial applications consist of swirl flow.

In previous work, the combustion characteristics of pulverized coal and biomass have been found. Ma et al. [1] presented the modelling methods for co-fired of pulverized coal and biomass in the furnaces. They showed that the model was able to predict the behavior of the biomass in the coal firing. Li et al. [2] studied devolatilization and char oxidize kinetics of torrefied biomass by experimental and computational fluid dynamics (CFD) modelling of co-firing with varying substitutions of pulverized torrefied-biomass in a pulverized coal steam generator. They found that torrefaction was able to provide a technical option for high substitution ratios of biomass in the co-firing with coal. Ma et al. [3] simulated the combustion of

biomass in existing pulverized coal fires furnace by using developed CFD model. The model result showed reasonably good agreement with experimental data. Li et al. [4] investigated combustion characteristics of pulverized torrefied-biomass firing with high-temperature air by experiment and CFD simulations. They reported the effect of drag force on volatilization of biomass and the flame characteristics. They also reported the effect of oxygen concentration in oxidizer and air velocity on flame characteristics. Yin et al. [5] investigated the combustion characteristics of firing pure coal and firing pure wheat straw in a 150 kW swirl-stabilized burner flow reactor under nearly identical conditions. Their results showed very dissimilar combustion characteristics between the coal flame and straw flame.

However, few studies have been done on the effect of swirl flow on the combustion characteristics of pulverized biomass. The purpose of this study was to investigate the combustion characteristics in a swirl burner for pulverized biomass. This investigation used CFD code to predict the effect of swirl number on the characteristics of biomass combustion by considering the flow, pressure and temperature field and specie concentration.

2. Method

Our method is similar to the method adopted by [4,6]. Following is the details of method use in this study. ANSYS Fluent CFD software was used to solve the discretized equation of combustion, fluid and solid particle flow and heat and mass transfer in the furnace [7]. A pulverized biomass furnace is shown in Figs. 1 and 2. The computational model of furnace represents a half of entire domain due to symmetry nature that

AEC0019

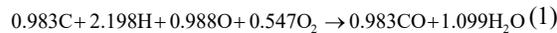
enable certain degree of simplification. Two dimensional computational domain and structured quadrilateral cells of mesh are used as presented in Fig. 3. The monitoring location of pulverized biomass furnace as illustrated in Fig. 4. The mesh independence was verified by comparing the axial velocity and temperature results as shown in Figs. 5 and 6, respectively. Mesh independence with 11568 cells is used for this simulation. The furnace operating conditions is given in Table 1. The proximate and ultimate analyses of pulverized biomass are given in Table 2. The distribution of pulverized biomass particle size is given in Table 3. In this work, the standard $k-\varepsilon$ model was used to model turbulent flow [8]. The radiative heat transfer included in simulation was the discrete ordinates (DO) model [9-11]. The absorption coefficient was calculate by weighted sum of gray gas model (WSGGM) [12,13].

2.1. Discrete phase model

For simulating the pulverized biomass, the discrete phase model (DPM) was employed by considering the Eulerian-Lagrangian method [7]. The gas phase was modelled by the Eulerian method, while the discrete solid phase of biomass particles was modelled by the Lagrangian method.

2.2. Combustion model

The single kinetic rate model was employed to predict the devolatilization of pulverized biomass [14]. The homogeneous combustion of gas phase using eddy-dissipation model [15]. Two-step global reaction of gas phase was modelled as follows:



The char oxidation was determined by the kinetic/diffusion-limited rate model [16,17]. The solid char surface oxidation model could be assumed as follows:



2.3. Nitric oxides model

Nitric oxide (NO_x) model consists of thermal NO_x , prompt NO_x and fuel NO_x . Thermal NO_x refers to the NO_x formed via the high temperature oxidation of the nitrogen of air in the combustion. As a matter of fact that prompt NO_x is generated by the reaction between nitrogen and hydrocarbon in fuel-rich zone of combustion [19]. Fuel NO_x is formed by the reaction between oxygen and nitrogen contained in the fuel [20]. In this study, the rate of thermal NO_x was calculated by the extended Zeldovich mechanism [18]. Fuel NO_x was assumed solely come from Nitrogen content in fuel.

2.4. Swirl number

The swirl number S of secondary air inlet of the burner defined as the ratio of tangential momentum flux to axial momentum flux. In this study it was calculated as [21]

$$S = \frac{\int_{R_i}^{R_o} W r \rho U 2\pi r dr}{R_o \int_{R_i}^{R_o} 2\pi r \rho U^2 dr} \quad (4)$$

where ρ is the air density, r is the radius of secondary air inlet, W is the mean azimuthal velocity, U the mean axial velocity, R_i is the inner radius of annular of secondary air inlet and R_o is the outer radius of annular of secondary air inlet. In order to investigate the effect of swirl number on combustion characteristics, swirl number was varied from 0.8 to 1.2 (0.8, 0.9, 1.0, 1.1, 1.2).

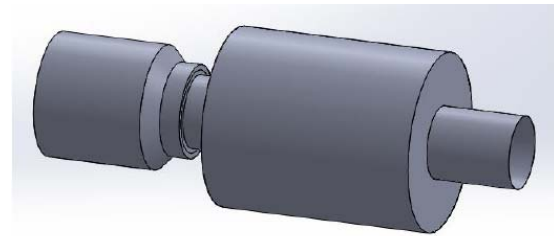


Fig. 1 Dimetric view of pulverized biomass combustion furnace.

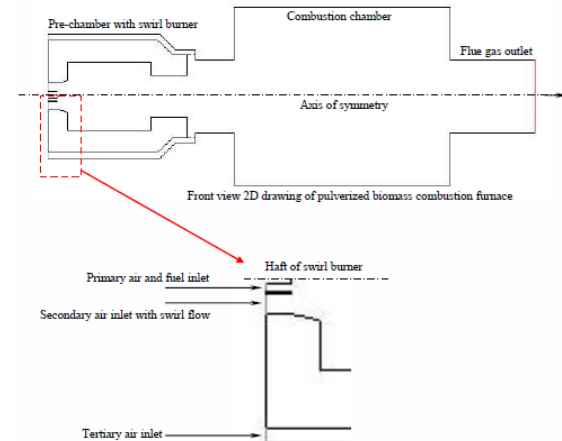
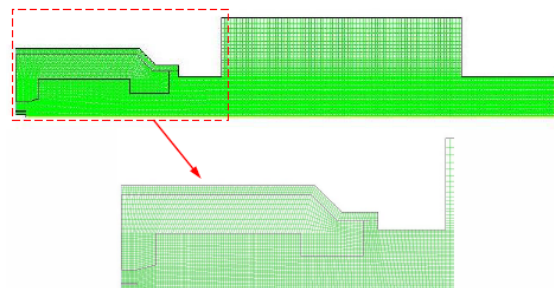


Fig. 2 The schematic of pulverized biomass furnace.



AEC0019

Fig. 3 The computational domain and mesh of pulverized biomass furnace.



Fig. 4 The monitoring location of pulverized biomass furnace, the radial position at T1=x=0.082 m, T2=x=0.182 m, T3=x=0.282 m, T4=x=0.382 m and T5=x=0.482 m from the burner and axial position at r=0.

Table. 1 Operating conditions of the furnace.

Thermal input based on fuel (kW)	500
Pulverized biomass feed rate at primary inlet (kg/s)	0.0317
Total excess air (%)	20
Primary air flow (kg/s)	0.0223
Primary air mass fraction	0.413
Primary air/Total air (wt%)	10
Secondary air flow (kg/s)	0.1449
Secondary air/Total air (wt%)	65
Swirl number of secondary air flow	0.8, 0.9, 1.0, 1.1, 1.2
Tertiary air flow (kg/s)	0.0557
Tertiary air/Total air (wt%)	25
Mole fraction of O ₂ in air inlet	0.21
Mole fraction of N ₂ in air inlet	0.79
Temperature of pulverized biomass inlet (K)	313
Temperature of primary, secondary and tertiary air inlet (K)	313
Temperature of combustion chamber wall (K)	773
Internal emissivity of combustion chamber wall (K)	0.75
Outlet pressure of flue gas (Pa)	-1500
Gravitational acceleration (m/s ²)	9.81
Operating pressure (Pa)	101325

Table. 2 Pulverized biomass analysis.

Proximate analysis (wt.%, as received)				
Ash	Volatile matter	Moisture	Fixed carbon	
2.28	76.68	5.81	15.23	
Ultimate analysis (wt.% Dry-Ash-Free)				
C	H	O	N	S
49.42	6.16	43.93	0.49	0
Higher heating value (HHV) 17500 kJ/kg				
Lower heating value (LHV) 16161 kJ/kg				

Table. 3 Pulverized biomass particle size distribution.

Particle size (μm)	% weight
500	2.6
362.5	16.8
240	25.5

165	12.6
112.5	18.1
37.5	24.4

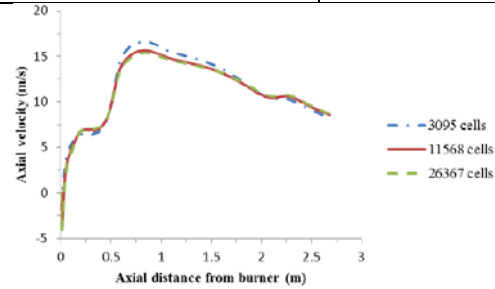


Fig. 5 Axial velocity along combustor axis at different grid sizes.

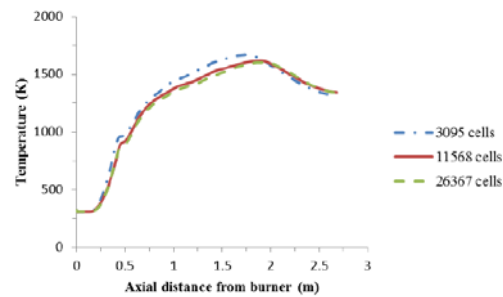


Fig. 6 Axial temperature along combustor axis at different grid sizes.

2.5. Pressure loss factor

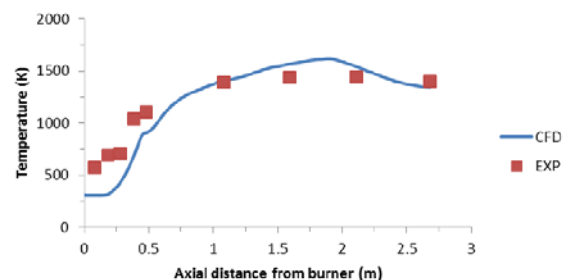
The pressure loss factor of the burner and furnace in this study was calculated as follows.

$$f = \frac{2 \Delta P}{\rho V_{avg}^2} \quad (5)$$

where ΔP is the pressure drop between secondary air inlet and flue gas outlet and V_{avg} is the average velocity of secondary air inlet.

2.6. Model validation

To obtain sensible prediction of the numerical results, the model was validated with the experimental results. Comparison between CFD and experimental data [22] on axial and radial temperature profile are shown in Figs. 7 and 8.



AEC0019

Fig. 7 Comparison of axial temperature between CFD and experimental results.

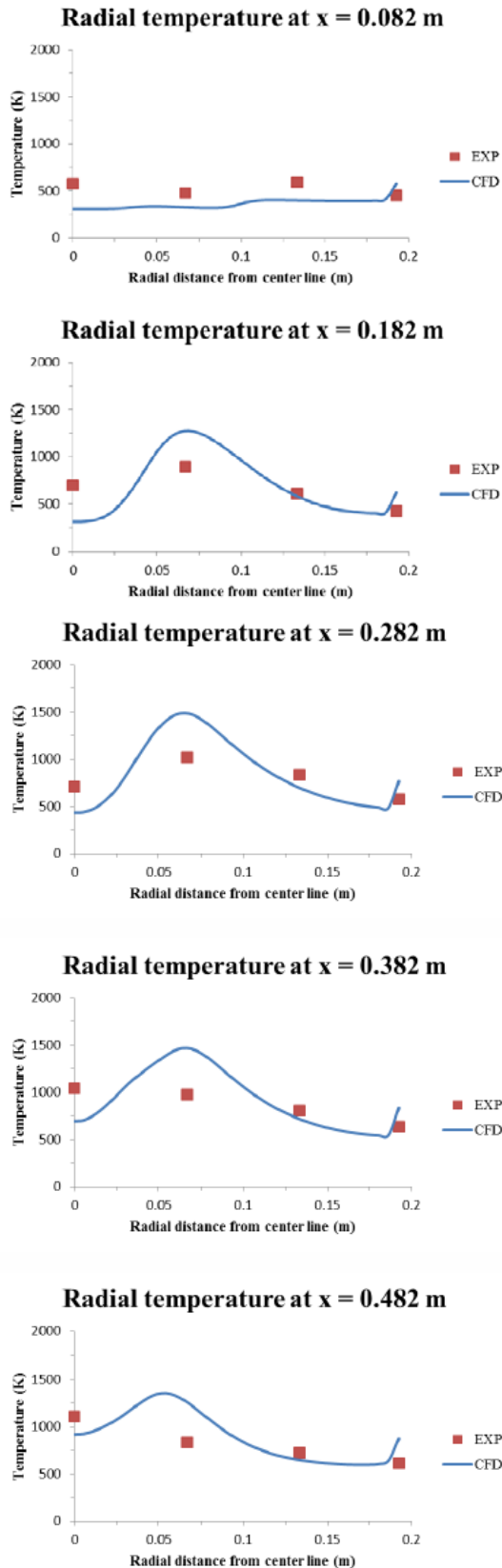


Fig. 8 Comparison of radial temperature between CFD and experimental results at 0.082, 0.182, 0.282, 0.382 and 0.482 m from the burner.

3. Results and discussion

This section describes numerical results of pulverized biomass combustion in the furnace at different swirl number from 0.8 to 1.2.

3.1. Axial velocity

Figure 9 shows the axial velocity contours at different swirl numbers. When swirl number increased, combustion was intensify by rapid mixing between fuel and secondary air, leading to significant increase in temperature and specific volume of the gas in the pre-chamber. As a result, axial velocity was found increased with this change. High velocity occurred at exit plane of pre-chamber to combustion chamber, especially at $S=1.2$, highest velocity magnitude of gas was observed.

3.2. Pressure distribution

Figure 10 compares the pressure distribution inside the furnace at different swirl numbers. When swirl number increased the pressure at pre-chamber was increased and greater area of negative pressure occurred at the connector between pre-chamber and combustion chamber. Higher swirl number require more pressure at the burner inlet to create stronger flow for the same mass flow rate. When swirl number increases the pressure loss factor also increase as shown in Fig. 11.

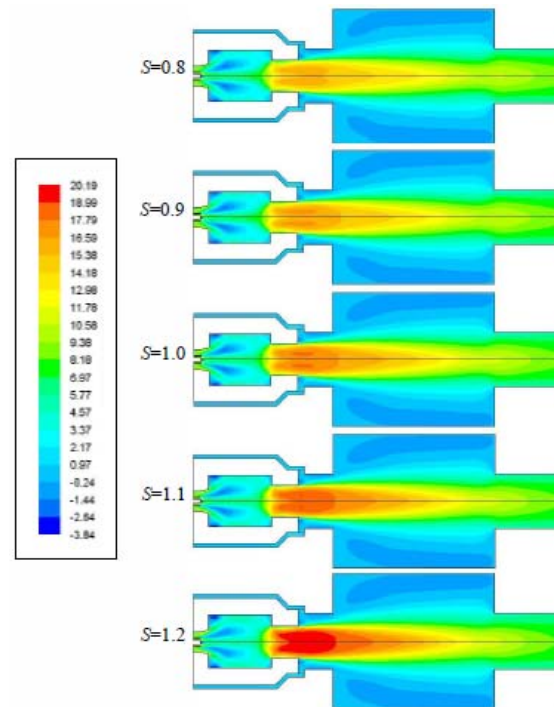


Fig. 9 Axial velocity (m/s) at different swirl numbers.

AEC0019

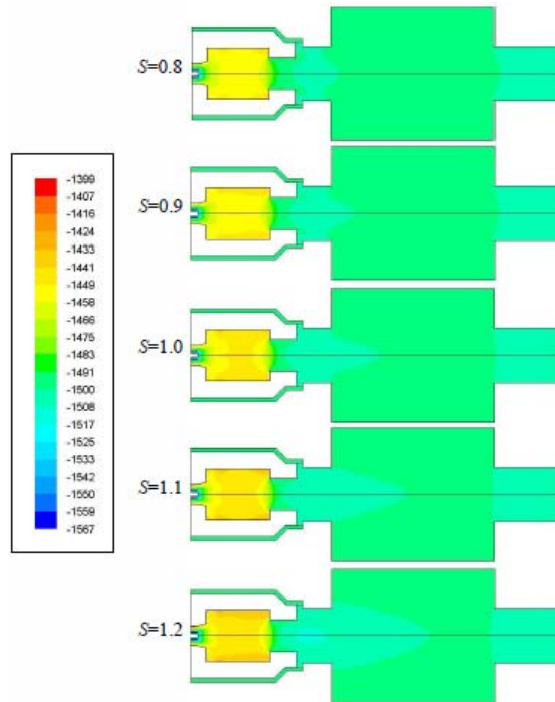


Fig. 10 Pressure (Pa) at different swirl numbers.

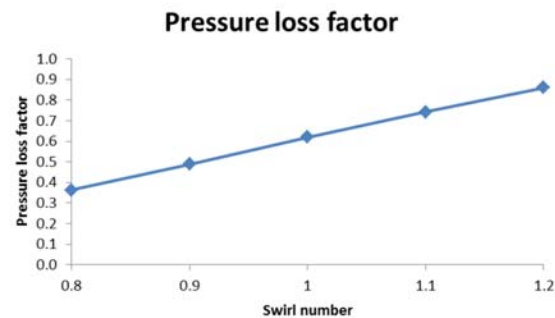


Fig. 11 Pressure loss factor at different swirl numbers.

3.3. Temperature distribution

Figure 12 displays the comparison of the temperature distribution inside the furnace at different swirl numbers. When swirl number increased from 0.8 to 1.2 the high temperature had shifted toward the inlet, especial at centerline, the temperature of combustion also increased. These temperature results may be explained by considering the high swirl number leading to stronger convection rapid mixing among fuel and air, rapid combustion took place near the burner.

3.4. Species concentration

Figure 13 presents the comparison of the concentration of volatile inside the furnace at different swirl numbers. When the swirl number increased the concentration of volatile also increased and the area of high volatile concentration was more apparent and moved nearer to the burner inlet, especially at centerline. The increase in volatile concentration indicated greater release rate due to higher temperature

created by the swirl number that enhance the flow magnitude and lead to higher mixing between air and fuel. This also affected to volatile reaction occurring at faster rate.

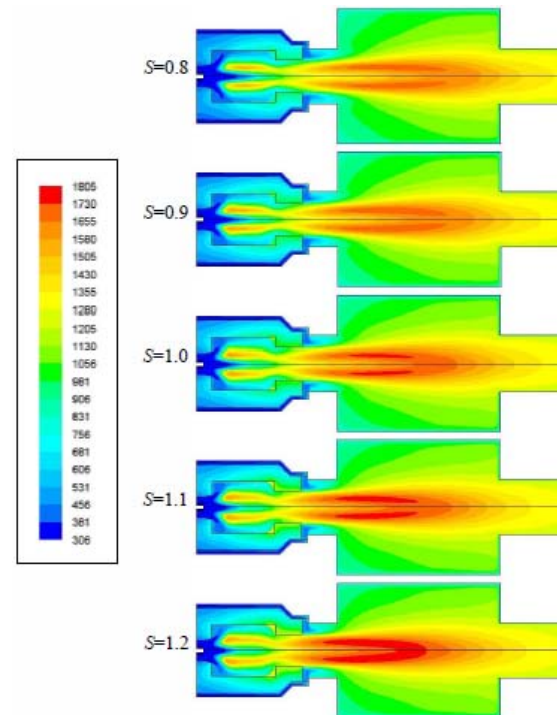


Fig. 12 Temperature (K) at different swirl numbers.

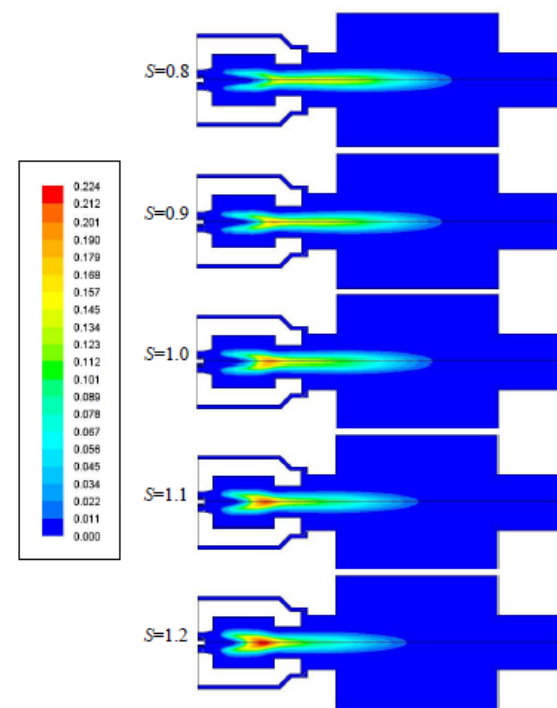


Fig. 13 Mole fraction of volatile at different swirl numbers.

AEC0019

Figure 14 shows the comparison of the oxygen (O_2) distribution inside the furnace at different swirl numbers. When the swirl number increased, rapid consumption of oxygen was observed as can be seen by oxygen distribution in the pre-chamber. The rapid consumption of oxygen can be explained by high swirl number increased the higher swirl flow leading to mixing between air and fuel and lead to faster reaction of combustion which more oxygen consumed.

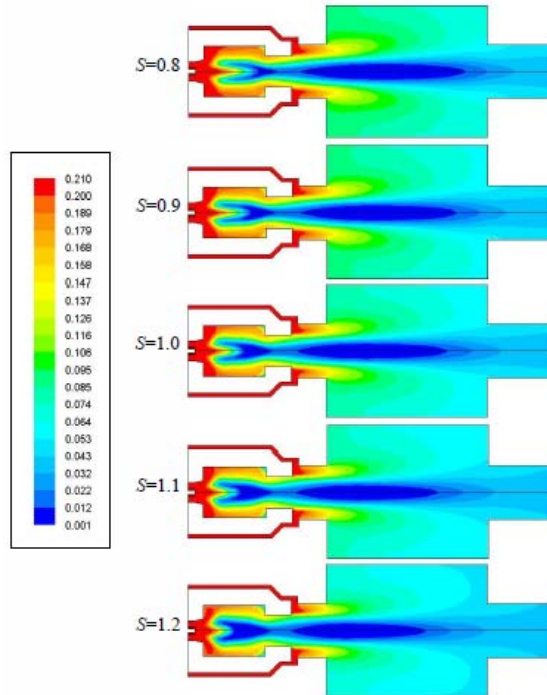


Fig. 14 Mole fraction of O_2 at different swirl numbers.

Figure 15 compares the concentration of carbon monoxide (CO) inside the furnace at different swirl numbers. At swirl number 0.8, 0.9 and 1.0 carbon monoxide could not completely combusted within the combustion chamber, carbon monoxide remain and left out from the combustion chamber through the flue gas outlet. When swirl number increased the combustion of carbon monoxide has been completely combusted. Therefore, greater swirl number results in greater consumption rate of carbon monoxide. At swirl number 1.1 and 1.2 the combustion of carbon monoxide completed. The rapid consumption of carbon monoxide can be explained by the same reason as described earlier in this section.

Figure 16 displays the carbon dioxide (CO_2) concentration inside the furnace at different swirl numbers. When swirl number increased the concentration of carbon dioxide was higher and occupied with relatively more uniform at the outlet zone. Effects of swirl on carbon dioxide distribution can also be described by faster rate of combustion upstream.

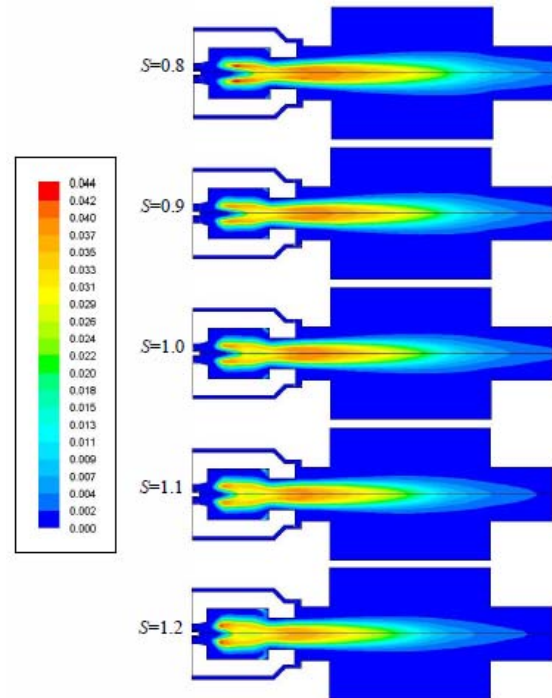


Fig. 15 Mole fraction of CO at different swirl numbers.

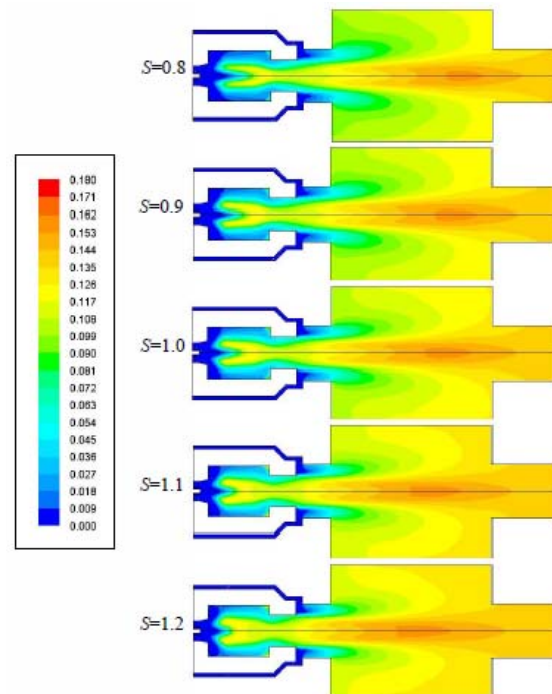


Fig. 16 Mole fraction of CO_2 at different swirl numbers.

3.5. NO_x formation

Figure 17 presents the comparison of the NO_x concentration inside the furnace at different swirl numbers. When swirl number increased from 0.8 to 1.1 the concentration of nitrogen oxide also increased.

AEC0019

The increase in NO_x was due to the increase in temperature causing greater production rate of thermal NO_x . However, NO_x concentration at outlet plane for swirl number 1.2 was lower than the cases with swirl number 1.0 and 0.9. This was partly due to dilution effect of flue gas. Investigation is under way to investigate the destruction mechanism of NO_x which is expected to play an important role on this result.

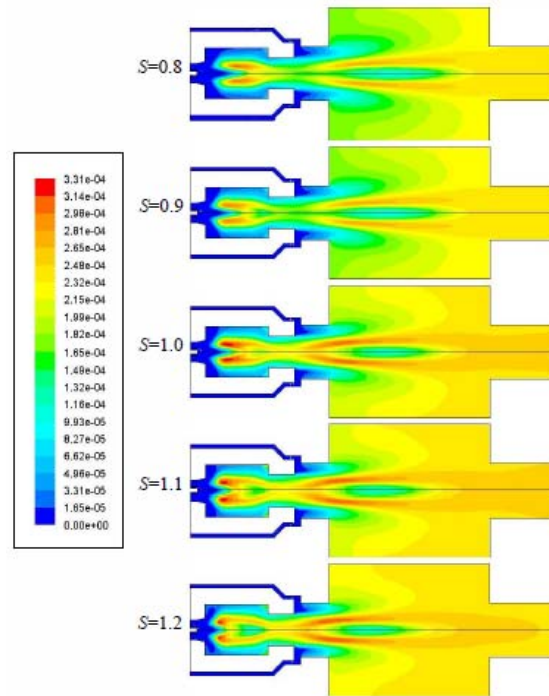


Fig. 17 Mole fraction of pollutant NO_x at different swirl numbers.

4. Conclusion

The numerical simulation of pulverized biomass combustion has been demonstrated to examine the effect of swirl number on combustion characteristics. The changes in flow field, pressure, temperature and species concentration were discussed. From the results, swirl number had important role in the combustion by improving the mixing of fuel and air stream and inducing the reverse flow. It can be concluded as follows:

At swirl number 0.8, 0.9 and 1.0, the pressure drop was relatively lower, resulting lower axial velocity. Carbon monoxide combustion was incomplete within the furnace and flow out of the calculation domain. NO_x concentration was relatively low for these swirl numbers.

At swirl number 1.1 more pressure drop was observed and axial velocity inside the furnace was relatively higher than those with swirl numbers 0.8, 0.9 and 1.0. Carbon monoxide combustion could be completed within the furnace. NO_x concentration was highest for this swirl number.

At high swirl number 1.2 which highest pressure drop and axial velocity inside the furnace. Carbon monoxide combustion could be completed within the furnace and consumed faster than swirl numbers 0.8, 0.9, 1.0 and 1.1. Lower NO_x concentration was found at swirl number 1.2 when compare with swirl numbers 1.0 and 1.1.

Acknowledgement

This research is financially supported by the Research and Researchers for Industries Program (RRI), The Thailand Research Fund.

References

- [1] Ma, M., Gharebaghi, R. Porter, Pourkashanian, M., Jones, J.M. and Williams, A. (2009). Modelling methods for co-fired pulverized fuel furnaces, *Fuel*, vol. 88(12), December 2009, pp. 2448–2454.
- [2] Li, J., Brzdekiewicz, A., Yang, W., and Blasiak, W. (2012). Co-firing based on biomass torrefaction in a pulverized coal boiler with aim of 100% fuel switching, *Applied Energy*, vol. 99, November 2012, pp. 344–354.
- [3] Ma, L., Jones, J.M., Pourkashanian, M. and Williams, A. (2007). Modelling the combustion of pulverized biomass in an industrial combustion test furnace, *Fuel*, vol. 86(12-13), August 2007, pp. 1959–1965.
- [4] Li, J., Biagini, E., Yang, W., Tognotti, L. and Blasiak, W. (2013). Flame characteristics of pulverized-biomass combusted with high-temperature air, *Combustion and Flame*, vol. 160(11), November 2013, pp. 2585–2594.
- [5] Yin, C., Rosendahl, L. and Kaer, S.K. (2012). Towards a better understanding of biomass suspension co-firing impacts via investigating a coal flame and a biomass flame in a swirl-stabilized burner flow reactor under same conditions, *Fuel Processing Technology*, vol. 98, June 2012. pp. 65–73.
- [6] Tu, Y., Liu, H., Chen, S., Liu, Z., Zhao, H. and Zheng, C. (2015). Numerical study of combustion characteristics for pulverized coal under oxy-MILD operation, *Fuel Processing Technology*, vol. 135, July 2015, pp. 80-90.
- [7] ANSYS, Inc., ANSYS Fluent On-line: www.ansys.com.
- [8] Launder, B.E. and Spalding, D.B. (1974). The numerical computation of turbulent flows, *Computer Methods in Applied Mechanics and Engineering*, vol. 3(2), March 1974, pp. 269-289.
- [9] Raithby, G. D. and Chui, E. H. (1990). A Finite-Volume Method for Predicting a Radiant Heat Transfer in Enclosures with Participating Media, *Journal of Heat Transfer*, vol. 112(2), 1 May 1990, pp. 415–423.
- [10] Chui, E. H., and Raithby, G. D. (1993). Computation of Radiant Heat Transfer on a Non-Orthogonal Mesh Using the Finite-Volume Method, *Numerical Heat Transfer, Part B: An International*

AEC0019

Journal of Computation and Methodology, vol. 23(3), 1993, pp. 269–288.

[11] Murthy, J.Y. and Mathur, S.R. (1998). A finite volume method for radiative heat transfer using unstructured mesh, Journal of Thermophysics and Heat Transfer, vol. 12, No. 3, July-September 1998, pp. 313-321.

[12] Smith, T. F., Shen, Z. F. and Friedman, J. N. (1982). Evaluation of Coefficients for the Weighted Sum of Gray Gases Model, Journal of Heat Transfer, Vol. 104(4), 1 November 1982, pp. 602–608.

[13] Coppalle, A. and Vervisch, P. (1983). The total emissivities of high-temperature flames, Combustion and Flame, vol. 49(1-3), January 1983, pp. 101–108.

[14] Badzioch, S. and Hawksley, P. G.W. (1970). Kinetics of Thermal Decomposition of Pulverized Coal Particles, Industrial and Engineering Chemistry Process Design and Development, vol. 9(4), October 1970, pp. 521–530.

[15] Magnussen, B.F. and Hjertager, B.H. (1977). On mathematical modeling of turbulent combustion with special emphasis on soot formation and combustion, Symposium (International) on Combustion, vol. 16(1), 1977, pp. 719-729.

[16] Field, M. A. (1969). Rate of Combustion of Size-Graded Fractions of Char from a Low Rank Coal between 1200 K–2000 K, Combustion and Flame, vol. 13(3), June 1969, pp. 237–252.

[17] Baum, M. M. and Street, P. J. (1971). Predicting the Combustion Behavior of Coal Particles, Combustion Science and Technology, vol. 3(5), 1971, pp. 231–243.

[18] Zeldovich, Y. B., Sadovnikov, P.Y. and Frank-Kamenetskii, D.A. (1947). Oxidation of Nitrogen in Combustion”, Publ. house of the acad. of Sciences USSR, 1947.

[19] Fenimore, C. P. (1971). Formation of nitric oxide in premixed hydrocarbon flames, Symposium (International) on Combustion, vol. 13(1), 1971, pp. 373-380.

[20] De Soete, G. G. (1975). Overall reaction rates of NO and N₂ formation from fuel nitrogen”, Symposium (International) on Combustion, vol. 15(1), 1975, pp. 1093-1102.

[21] Sheen, H. J., Chen, W. J., Jeng, S. Y. and Huang, T. L. (1996). Correlation of swirl number for a radial-type swirl generator, Experimental Thermal and Fluid Science, vol. 12(4), May 1996, pp. 444-451.

[22] C. Turakam, (2015), Biomass burner development in industrial boilers, Master Thesis, Faculty of Engineering, King’s Mongkut Institute of Technology Ladkrabang.